Journal of Aridland Agriculture 2025, 11: 83-92
doi: 10.25081/jaa.2025.v11.9627
https://updatepublishing.com/journal/index.php/jaa

Research Article

ISSN: 2455-9377

Environmental and spectroscopic approaches to lead ion detection using Schiff base in arid and semi-arid zones

P. Nivetha, S. Abinaya, A. Thangamani*

Department of Chemistry, Karpagam Academy of Higher Education, Eachanari, Coimbatore-641021, Tamil Nadu, India

Received: February 13, 2025
Revised: June 11, 2025
Accepted: June 12, 2025
Published: June 27, 2025

***Corresponding author:**
A. Thangamani
E-mail: tangabell2003@gmail.com

ABSTRACT

A novel colorimetric chemosensor, (E)-2-methoxy-3-((naphthalen-1-ylamino)methylene)chroman-4-one (FCNA), has been successfully developed for the selective detection of lead (Pb^{2+}) ions in environmental soil samples such as those from arid land and semi-arid land. This sensor exhibits high sensitivity and selectivity, with a low detection limit of 5.24×10^{-10} M and an association constant of 3.22×10^{5} M^{-1}, confirming its strong binding affinity toward Pb^{2+} ions. Structural analysis via FTIR, NMR, and Job's plot suggests the formation of stable 2:1 complex between FCNA and Pb^{2+}, reinforcing its specificity. The ease of synthesis and robust selectivity make FCNA an ideal candidate for Pb^{2+} ions detection, particularly in environmental soil monitoring. Real sample analysis was conducted to validate its performance, demonstrating high reliability in detecting Pb^{2+} ions in complex matrices. Given its exceptional detection ability, FCNA emerges as a promising tool for heavy metal ion monitoring, supporting environmental safety assessments and pollution control efforts in soils.

KEYWORDS: Arid and semi-arid soil, Lead ion, Chemosensor, Schiff base

INTRODUCTION

Transition metal ions play a crucial role in biological systems, environmental balance, and industrial activities. While essential for various physiological functions, their excess or deficiency can lead to serious health and ecological consequences. Beyond human health, transition metal ions significantly impact the environment (Durgaparameshwari *et al.*, 2024; Santhamoorthy *et al.*, 2024). Industrial pollution, including heavy metal contamination from mining, manufacturing, and chemical waste disposal, introduces large amounts of toxic metal ions into water bodies and soil. These pollutants disrupt ecosystems, harming aquatic life and food chains. Bioaccumulation of heavy metals in living organisms can lead to long-term ecological damage, affecting reproductive and developmental health in wildlife (Xiang *et al.*, 2006; Wang *et al.*, 2017a; Roy *et al.*, 2019).

Arid and semi-arid regions make up nearly 40% of the Earth's land surface, where agriculture remains a vital means of sustenance for local populations. However, farming in these areas is fraught with challenges, including extreme temperatures, limited water availability, barren soil, frequent droughts, and wind erosion. Additionally, the fragile topography makes these regions highly susceptible to natural disasters (Hussain *et al.*, 2025). Since rainfall is insufficient to support consistent agricultural productivity, supplementary irrigation becomes essential for sustaining crop growth. To address water scarcity, many communities in these regions resort to wastewater recycling for irrigation. However, soil salinity presents another significant hurdle, threatening soil health and reducing agricultural yield. Due to the adverse effects on human health and the environment, it has become essential to create selective and sensitive structures for measuring the concentrations of hazardous heavy metal ions nowadays (Burla *et al.*, 2013; Joshi, 2016; Suaad *et al.*, 2020).

One of the main objectives in the field of chemical sensors at the moment is the identification and detection of metal ions that are significant to both the environment and biology using chemosensors (Wang *et al.*, 2017b). Among the methods of chemosensors colorimetric detection is one of the simplest way of detection of metal ions with low cost equipments (Chen & Huang, 2002; Prabhu *et al.*, 2015; Rahimi *et al.*, 2020). More significantly, the majority of colorimetric chemosensors are capable of "naked eye" detection, which elevates the sensing approach above alternative analytical techniques like conventional instrumental detection methodologies (Amini *et al.*, 2020; Rupa *et al.*, 2022).

Copyright: © The authors. This article is open access and licensed under the terms of the Creative Commons Attribution License (http://creativecommons.org/licenses/by/4.0/) which permits unrestricted, use, distribution and reproduction in any medium, or format for any purpose, even commercially provided the work is properly cited. Attribution — You must give appropriate credit, provide a link to the license, and indicate if changes were made.

Pb^{2+} is one of the most hazardous metal ions among the heavy metals even in a low concentration (Kuo *et al.*, 2007; Rasmussen *et al.*, 2015; Sun *et al.*, 2017). The discharge of industrial waste effluent indicates that Pb^{2+} is one of the most dangerous metal ions naturally occurring in the environment, water, and agricultural land. So it is widely acknowledged that Pb^{2+} is non-degradable and easily deposited in food and water (Velmathi *et al.*, 2011; Udhayakumari & Velmathi, 2013; Lan *et al.*, 2017). Pb^{2+} has a major negative impact on human health and is a contaminant in the environment, hence it needs to be determined at sub-micro levels in a variety of matrices using a technology that is precise, sensitive, and selective. World Health Organization (WHO) guidelines state that the maximum amount of lead in drinking water is 10 µg/L (Cho *et al.*, 2018; Pothulapadu *et al.*, 2021). According to the US Environmental Protection Agency (EPA) and the Bureau of Indian Standards, the acceptable limit for this substance is 0.05 mg L^{-1} and 0.1 mg L^{-1}, respectively, due to the toxicity of lead (Choi *et al.*, 2014).

Due to the photochemical properties of chromone moiety it is used in chemosensors to determine different analytes (Łukasik *et al.*, 2016; Dwivedi *et al.*, 2020). Therefore, we synthesize chromone Schiff base. It is predominantly used in research such as analytical, optical sensors, biological and industrial application due to the presence of oxygen (Cave *et al.*, 2000). Schiff base structures yield unique selectivity, sensitivity, and stability for a particular ion while providing geometric control over host-guest interactions such as hydrogen bonding, metal-receptor coordination, electrostatic force, van der Waals forces, and hydrophobic interactions (Tahmasebi *et al.*, 2014). As of right now, chemosensor advancements for metal ion detection are quite important and it is made up of a signal transducer and a receptor (Torawane *et al.*, 2015; Li *et al.*, 2022). Noncovalent interactions between the receptor and the analyte facilitate interaction, and the signal transducer records these interactions as modifications to the analyte's optical or electronic features (Shoora *et al.*, 2015).

EXPERIMENTAL METHODS

The formyl chromone were prepared by previously reported Vilsmeier-Haack method. The alpha naphthylamine were purchased from Sigma Aldrich. Methanol was used as the solvent for the reaction and recrystallization. The metal salts were purchased from Loba chemicals, here we used chlorides and nitrates salts for sensing studies.

The FT-IR spectra were recorded in Bruker Spectrometer (ATR mode) in the range of 550 to 4000 cm^{-1}. The fluorescence and UV/Visible Spectra were recorded in Horiba FluoroMax Spectrofluorometer (USA) and JASCO 750 UV-Vis Spectrophotometer (Japan) with quartz Cuvette (path length=10 mm). A space should be given between the 10 and mm. The NMR (both proton and carbon) were recorded in Brukner 400 MHz.

Synthesis and Characterization of the Probe (FCNA)

3- formyl chromone (2mmol) were dissolved in 10 mL of methanol in conical flask. The methanolic solution of 1-naphthylamine (2mmol) were slowly added to the conical flask and stirred for 6 hours. After completion of the reaction yellow colour solid was formed, filtered the solid precipitate and washed with cold methanol, and recrystallized with hot methanol (Figure 1). FT-IR (ATR Mode cm^{-1}): 1641 (C=O), 1605 (C=C), 1289 (C-N).^{1}H NMR (ppm, $CDCl_3$): 13.01 (H-12) (d, 1H, NH), 8.19 (H-5) (d, 1H, *J*=8.4Hz), 8.06 (H-4') (dd, 1H, *J*=7.6 &1.6 Hz), 7.85 (H-8') (d, 1H, *J*=8 Hz), 7.70 (H-11) (s, 1H), 7.67-7.57 (H-6'&H-7') (m, 2H,), 7.55-7.51 (H-6) (m, 1H), 7.49-7.41 (H-3'&H-4') (m, 2H), 7.29 (H-2') (d, 1H, *J*=7.6 Hz), 7.15-7.11 (H-7) (m, 1H), 7.06 (H-8) (d, 1H, *J*=8 Hz), 5.73(H-2) (s,1H), 3.53 (OCH_3) (s, 3H). ^{13}C NMR (ppm, $CDCl_3$): 181.51 (C-4), 155.76 (C-9), 145.52 (C-11), 135.92 (C-1'), 134.39 (C-7), 120.94 (C-8), 128.52, 126.97, 126.79, 126.37 (C-5), 125.70,124.97, 124.94, 122.94, 122.24 (C-6), 120.94, 117.94, 117.-94, 104.94 (C-2'), 101.72 (C-2),55.2 (OCH_3').

Preparation of Solutions for Spectral Studies

For sensing studies, the stock solution of FCNA was prepared as $1x10^{-3}$ M in 9:1 (v/v) CH_3OH: H_2O. Metal ion solution was prepared as $1x10^{-3}$ M in 9:1 (v/v) CH_3OH: H_2O. Same solutions were used for fluorescent spectral studies.

DFT Calculation

The DFT studies were done by using gaussian 5.0. The probe FCNA and FCNA-Pb^{2+} Complex were optimised and the energy was calculated by using Becke's three parameter Lee-Yang-Parr (B3LYP) and basic set is 6-31G. The FMO also calculated for better understand of the probe and complex.

Application

The synthesised probe FCNA was selectively detect the Pb^{2+} ions in the solution state by changing the visual colour change from yellow to Colourless, which were observed in paper strip.

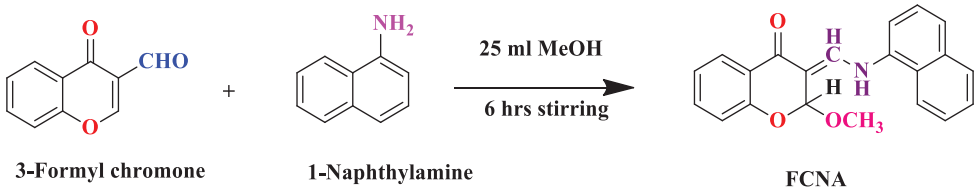

Figure 1: Synthesis of FCNA

RESULTS AND DISCUSSION

Chemistry

The chromone based Schiff base (FCNA) was synthesized by stirring the solution of 3- formyl chromone (1 mmol) and 1-naphthylamine (1 mmol) in methanol for 6 hrs (Figure 1). Were that the 2nd position of 3- formyl chromone was undergo *in-situ* nucleophilic substitution takes place in methoxide ion *via* solvent (Figure 2). The synthesized compound was characterized by FT-IR, ^{1}H NMR and ^{13}C NMR spectral technique. The appearance of the peak in ^{1}H NMR (Figure 3) at 13.01 ppm due to N-H proton and 7.70 ppm due to imine proton of the chromone ring confirmed the structure of the chemosensor. The peaks at 3.53 ppm and 5.73 ppm are due to OCH_3 attached to H-2 proton and methine proton (H-2) respectively. The appearance of a peak in ^{13}C NMR (Figure 4) at 55.50 ppm due to OCH_3 and 101.72 ppm due to methine carbon (C-2) confirmed the structure of the above chemosensor. The peaks at 181.51 ppm and 145.52 ppm are due to carbonyl carbon (C-4) of the chromone moiety and imine CH carbon (C-11). In the FT-IR spectrum (Figure 5) of FCNA bands at 1641, 1605 and 1289 cm^{-1} are due to C=O, C=C and C-N groups respectively (Maurya & Singh, 2017).

UV-Vis Spectral Response of Probe (FCNA)

The colorimetric response of the probe (FCNA) was initially examined by preparing stock solutions of the probe and metal ions at 1×10^{-3} M in 10 mL of PBS buffer (pH=7.2). From this stock, 100 µL of the probe was mixed with various metal ions (Ag^{+}, Al^{3+}, Bi^{3+}, Ca^{2+}, Cd^{2+}, Co^{2+}, Cr^{3+}, Cu^{2+}, Hg^{2+}, Na^{+}, Ni^{2+}, Zn^{2+}, Pb^{2+}) under identical conditions. Upon the addition of each metal ion, distinct color changes were observed; however, only Pb^{2+} ions caused a transition from yellow to colorless, as illustrated in Figure 6. Under similar experimental conditions, spectral analysis was performed to investigate the probe's optical response. The FCNA probe exhibited an absorbance

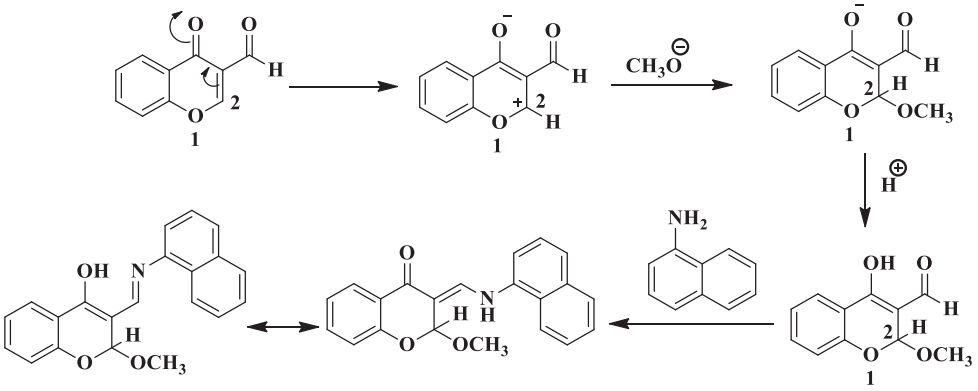

Figure 2: *In-situ* nucleophilic substitution of methoxide ion in 3- formyl chromone followed by simple condensation reaction FCNA

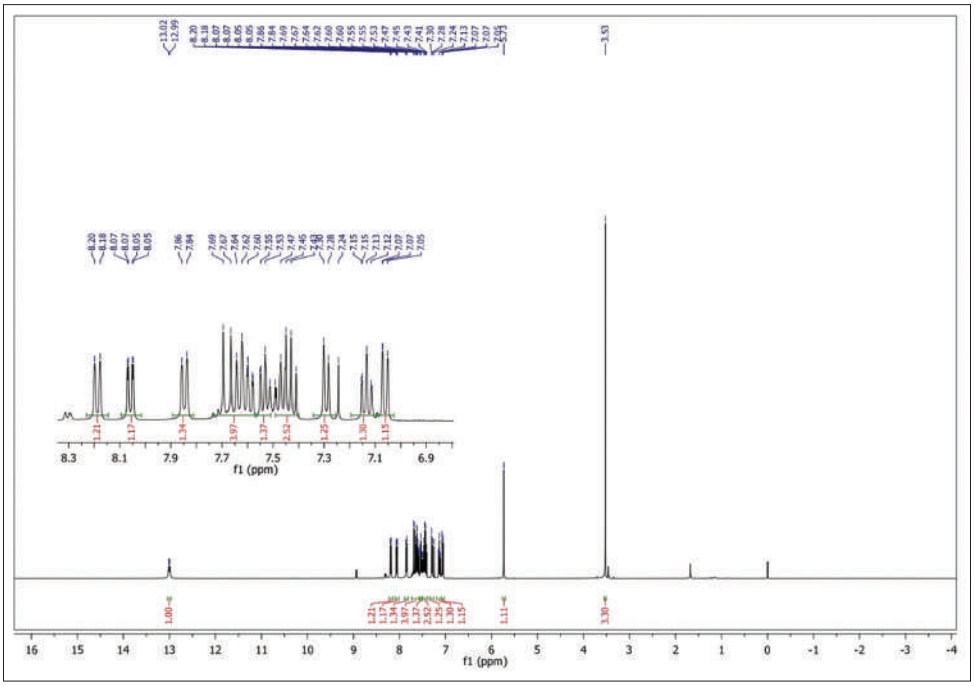

Figure 3: ^{1}H NMR of FCNA

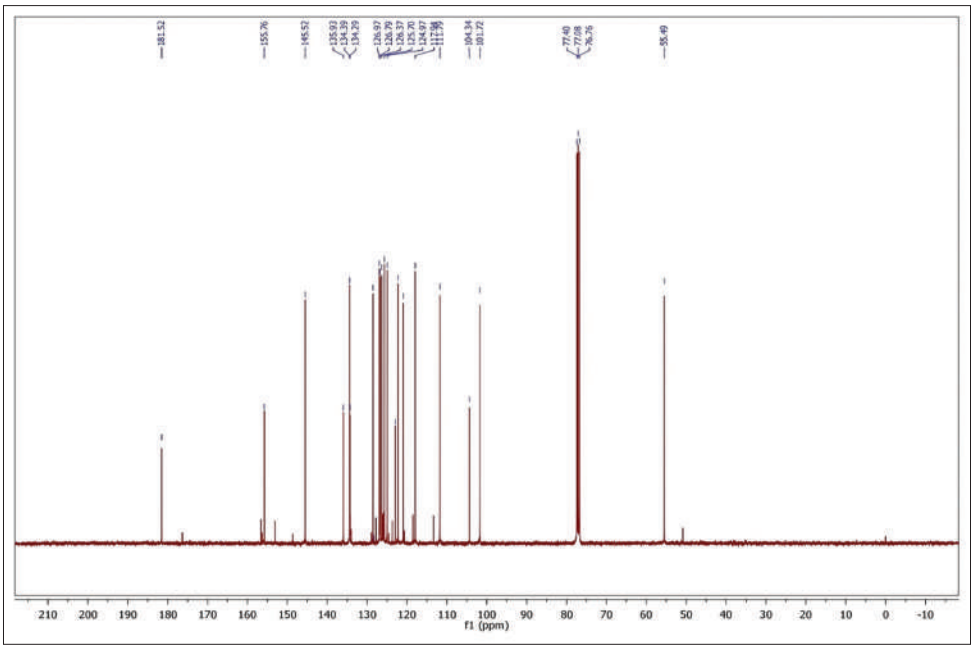

Figure 4: ^{13}C NMR of FCNA

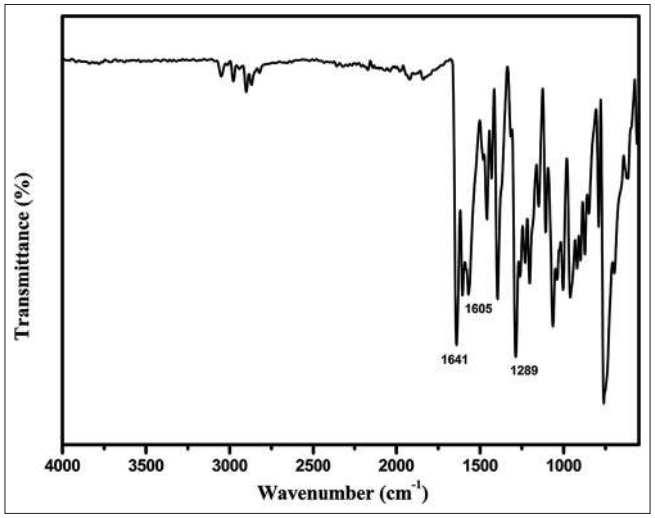

Figure 5: FT-IR spectrum of FCNA

band at 398 nm, attributed to the π-π* transition. Upon the gradual addition of Pb^{2+} ions, a new absorbance peak appeared at 288 nm, indicating a blue shift. Concurrently, absorbance at 398 nm decreased, while 288 nm absorbance increased, leading to the formation of an isobestic point at 335 nm, which signifies complex formation in the liquid state. During the measurement, Pb^{2+} ions were added up to 1.8 equivalents to the FCNA solution, with results presented in Figure 7 (Caballero *et al.*, 2008).

Fluorescence Studies on FCNA

Fluorimetric titrations were conducted to further investigate the sensing behaviour and properties of FCNA toward Pb^{2+} ions. Fluorescent emission was analysed in the presence of various cations (Ag^{+}, Al^{3+}, Bi^{3+}, Ca^{2+}, Cd^{2+}, Co^{2+}, Cr^{3+}, Cu^{2+}, Hg^{2+}, Na^{+}, Ni^{2+}, Zn^{2+}, Pb^{2+}) using PBS buffer (pH=7.2) as the medium. FCNA exhibited fluorescent bands at 445 nm and 353 nm (with excitation at 300 nm). Upon the addition of different cations, no significant change in fluorescence intensity was observed, except in the case of Pb^{2+} ions, which demonstrated a notable enhancement at 445 nm. To quantify this response, titration experiments were carried out, revealing a gradual increase in fluorescence intensity up to 1.7 equivalents of Pb^{2+}. Beyond this point, fluorescence enhancement stabilized at 2.0 equivalents, indicating saturation. Despite the substantial increase in fluorescence observed spectroscopically, there was no visible fluorescence color change detected during the experiment. Figure 8 illustrates the fluorescence intensity variations, highlighting the selective and enhanced response of FCNA toward Pb^{2+} ions compared to other competing metal ions. This strong specificity suggests FCNA as a promising probe for lead ion detection, particularly in complex environments (Elkhatib & Moharem, 2015).

Interference Experiments

The selectivity of the FCNA for Pb^{2+} ions was evaluated through competitive titrations, conducted both in the absence and presence of lead (II) ions. To ensure accuracy, 1:1 solutions of the probe with various concentrations of competing cations were prepared and tested. These titrations provided insight into the specific interaction between FCNA and Pb^{2+}, determining its effectiveness in detecting lead ions without significant interference from other metal ions. As depicted in Figure 9, the selectivity of FCNA for Pb^{2+} ion was confirmed through fluorescence emission at 445 nm. The fluorescence intensity exhibited a distinct response upon the introduction of Pb^{2+} ion, while the presence of other competing cations produced only negligible variations in the emission spectrum. This result demonstrates the strong preference of FCNA for Pb^{2+}, suggesting that it has an excellent ability to discriminate lead

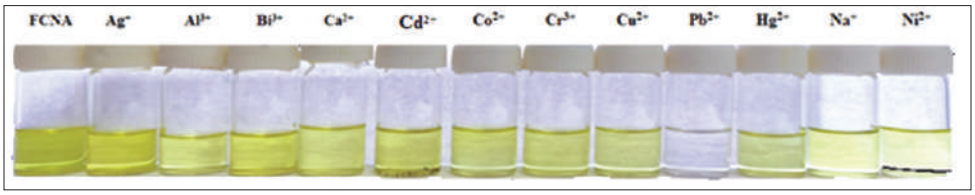

Figure 6: Naked visual colour changes of FCNA with metal ions

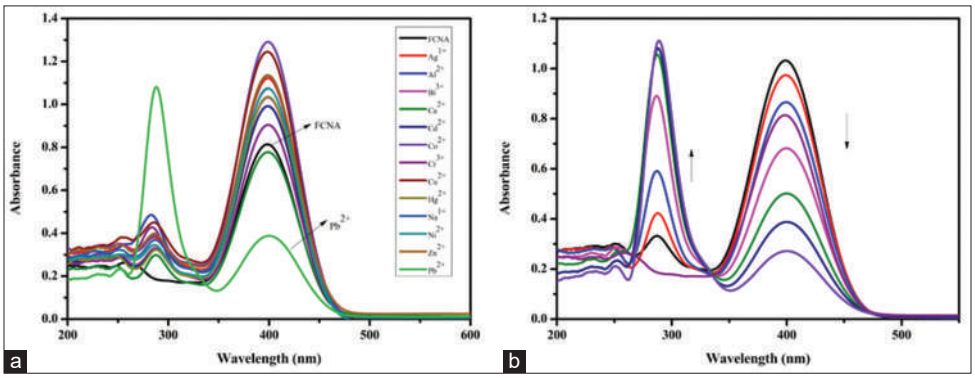

Figure 7: (a) UV-vis spectra of FCNA with metal ions in presence of PBS buffer in EtOH. (b) UV titration of Pb2+ ions with FCNA in presence of buffer upto 1.8 equivalents

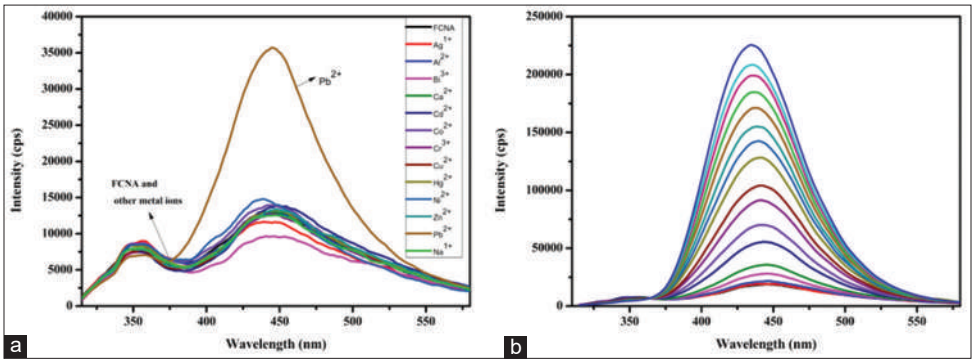

Figure 8: (a) Fluorescent spectra of FCNA with metals at excitation 300 nm. (b) Fluorescent titration of Pb^{2+} ions with FCNA up to 2 equivalent

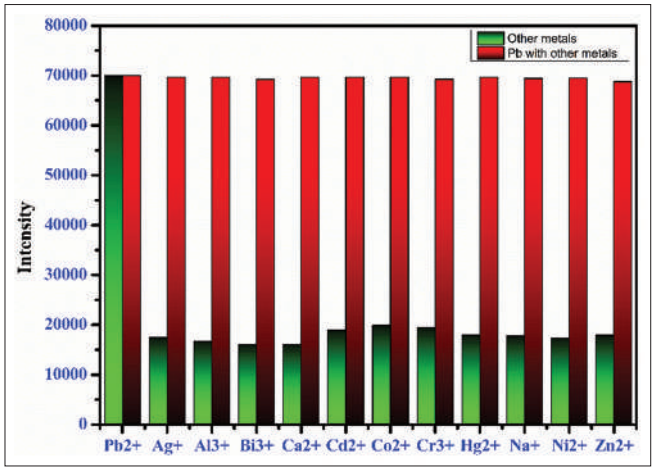

Figure 9: Relative fluorescence emission intensity of FCNA in the presence of various metal ions in presence of PBS buffer

ions from a complex mixture of metals (Sun *et al.*, 2012; Leslee *et al.*, 2018; Maloney *et al.*, 2018).

Jobs Plot Measurement

To analyse the binding performance of FCNA with Pb^{2+} ion, fluorescence measurements were conducted using the Job's plot (continuous variation method) to determine the stoichiometry of the interaction. The fluorescence intensity reached its maximum at 445 nm when the mole fraction was 0.2, indicating that the formation of the FCNA-Pb^{2+} complex follows a 2:1 stoichiometric ratio. This result suggests that two FCNA molecules effectively coordinate with a single Pb^{2+} ion, leading to optimal fluorescence enhancement. As shown in Figure 10, this strong binding interaction highlights FCNA's selectivity and effectiveness as a chemosensor for Pb^{2+} detection (Novikov, 2022).

Effect of pH Studies

pH plays a significant role in the Pb^{2+} sensing ability of FCNA, as illustrated in Figure 11. Fluorescence responses of FCNA to Pb^{2+} ion was evaluated across various pH levels to determine the optimal pH range for the FCNA–Pb^{2+} system. The emission

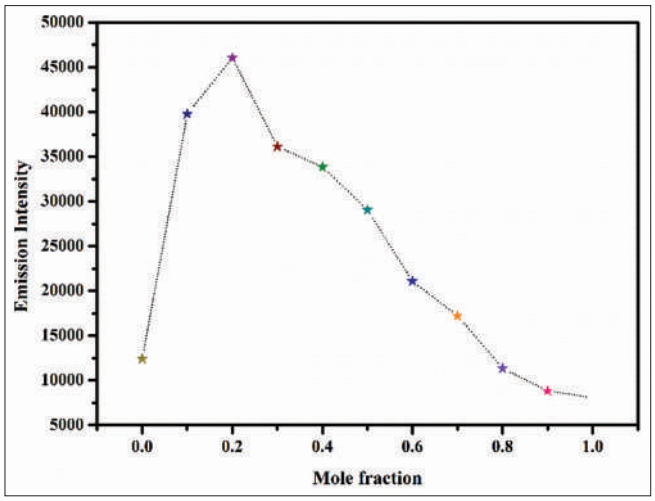

Figure 10: Job's plot for FCNA with Pb^{2+} ion according to continuous variation method

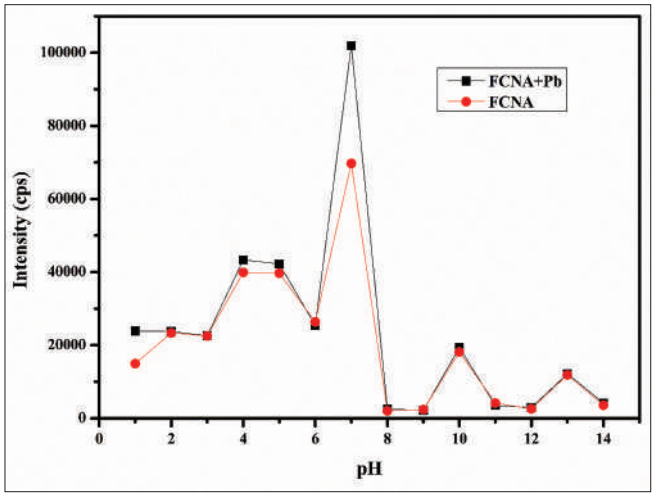

Figure 11: Effect of pH with FCNA and Pb^{2+} ion in different pH levels at emission band at 445 nm upon the excitation 300 nm

intensity of FCNA remained relatively stable between pH 1 and 7, showing a slight increase in fluorescence. However, upon the addition of 1 equivalent of Pb^{2+} ion, the fluorescence intensity at pH 7 was noticeably enhanced compared to other pH levels. These findings indicate that the FCNA–Pb^{2+} complex operates effectively at neutral pH, confirming its environmental sustainability and suitability for analysing real-world environmental samples. The ability to function under neutral conditions makes FCNA a promising chemosensor for lead ion detection in diverse aqueous systems.

Determination of Detection Time of FCNA and Pb^{2+}

In Figure 12, the effect of reaction time on the fluorescence spectra of the detection solution was examined. FCNA was introduced with 1 equivalent of Pb^{2+} ions, and fluorescence intensity was monitored at 446 nm at 1-minute intervals. The emission intensity gradually increased over time, indicating progressive binding between FCNA and Pb^{2+}. After 14 minutes, the fluorescence

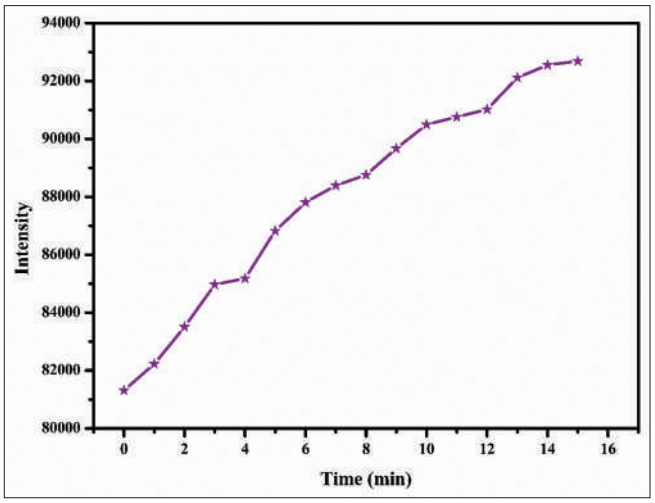

Figure 12: Time response ability of FCNA with Pb^{2+} ion in EtOH solution

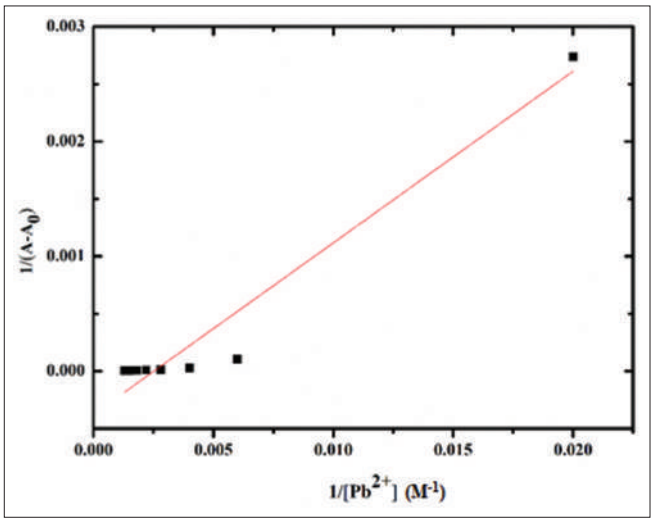

Figure 13: Binding constant calculated by using Benesi–Hildebrand (B-H plot)

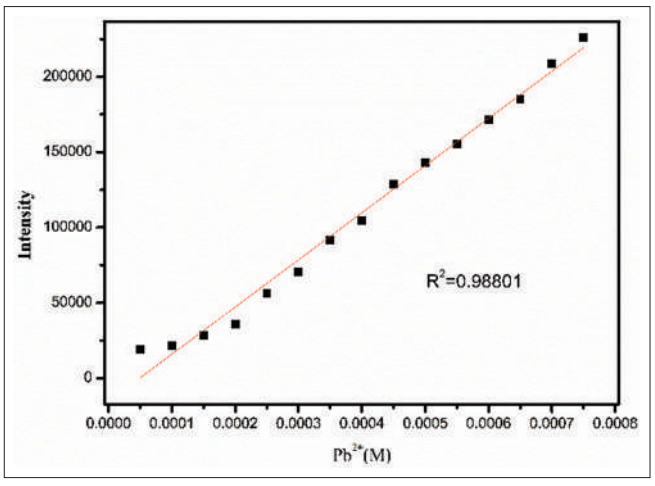

Figure 14: Limit of detection of FCNA with Pb^{2+} ion

intensity reached its maximum and saturated, signifying a strong binding interaction between FCNA and Pb^{2+} ion. This result

suggests that the complex formation occurs efficiently within this timeframe. However, a reversibility study was not feasible, indicating that the interaction might be irreversible or kinetically slow in dissociation under the given conditions. These findings emphasize the binding stability of FCNA with Pb^{2+} ion, making it a promising candidate for selective Pb^{2+} detection.

Binding Constant

The binding constant (Ka) of FCNA with Pb^{2+} ion was calculated from Benesi–Hildebrand (B-H Plot) using the following equation.

$$\frac{1}{(A-Ao)} = \frac{1}{K_a(A_{max}-A_o)[Pb^{2+}]} + \frac{1}{(A_{max}-A_o)}$$

Where, is the intensity of probe FCNA, A is the observed intensity in the addition of concentration of Pb^{2+} ion, is the emission intensity at saturation point of Pb^{2+}, K_a is the association constant and Pb^{2+} is the receptor. By using the equation, binding constant is determined as $3.22\times10^{5}M^{-1}$ in Figure 13 (Leslee *et al.*, 2018).

Measurement of Detection Limit

In Figure 14, the limit of detection (LOD) was calculated by using the following equation.

$$LOD = \frac{3\sigma}{K}$$

Where, σ is the standard deviation of the probe and K is the slope which is calculated between the intensities and concentration of metal ions. Through the measured values LOD was found to be $5.24x10^{-10}$ M (Leslee *et al.*, 2018).

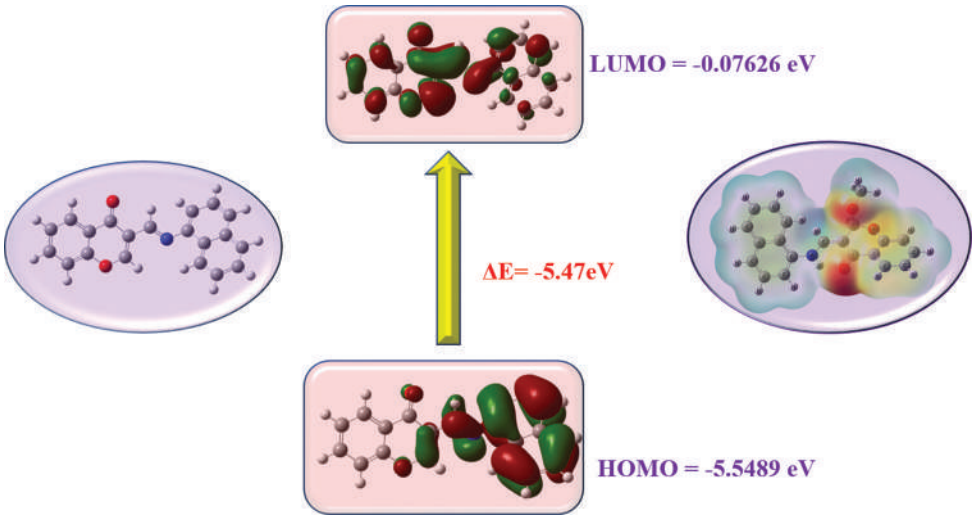

Figure 15: The fully optimized structure of FCNA and FMO orbital of FCNA and ESP

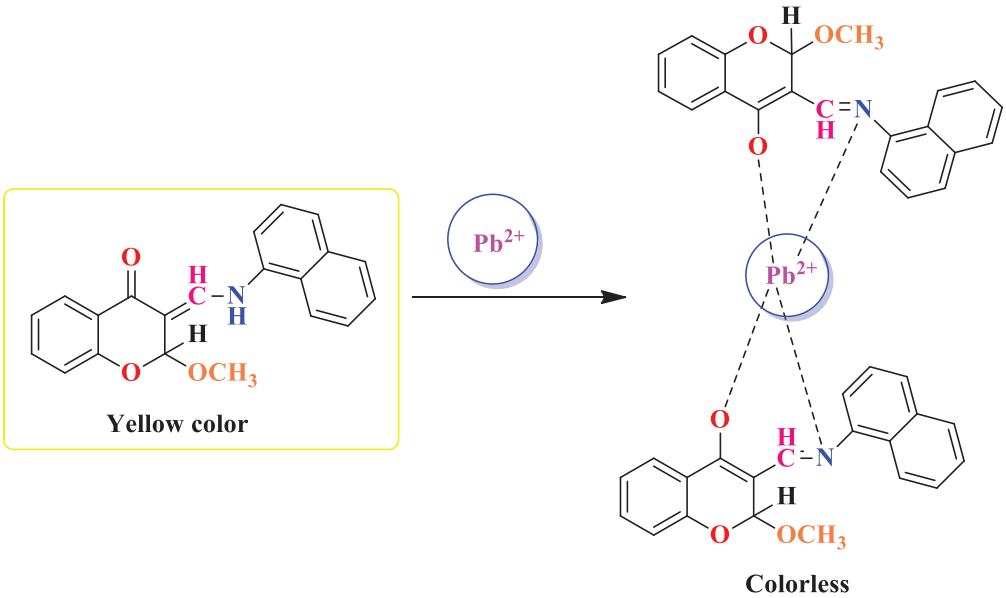

Figure 16: A plausible mechanism of FCNA with Pb^{2+}ion

DFT Computational Studies

To gain deeper insight into the interaction between Schiff base FCNA, both experimental and theoretical calculations were performed using Gaussian 9.0. The calculations were carried out using Becke's three-parameter Lee-Yang-Parr (B3LYP) functional, along with the 6-31G basis set, ensuring accurate energy estimations and structural optimization. The fully optimized molecular structure of FCNA was obtained and analysed, as shown in Figure 15, to determine its electronic configuration and stability. Additionally, Frontier Molecular Orbital (FMO) calculations were conducted to examine the electronic properties of FCNA, particularly the Highest Occupied Molecular Orbital (HOMO) and Lowest Unoccupied Molecular Orbital (LUMO) energy levels. These FMO analyses help in understanding the charge transfer and interaction behaviour of FCNA when binding with Pb^{2+} ion, confirming its effectiveness as a colorimetric sensor.

Plausible Sensing Mechanism of FCNA and Pb^{2+} Ion

The plausible sensing mechanism was examined, where the shift in the imine peak indicated the binding interaction between FCNA and Pb^{2+} ion. The sensing mechanism follows an Intramolecular Charge Transfer (ICT) process, involving electron transfer from the keto to enol form upon interaction with Pb^{2+} ion (Sun *et al.*, 2012). Further confirmation was conducted using the continuous variation method (Job's plot), which clearly demonstrated that the complex forms in a 2:1 ratio (FCNA: Pb^{2+}). Additionally, a Benesi–Hildebrand (B-H) plot was generated to determine the association constant of the FCNA–Pb^{2+} complex, reinforcing the strong binding affinity between the sensor and the metal ion. The formation of the complex is illustrated in Figure 16.

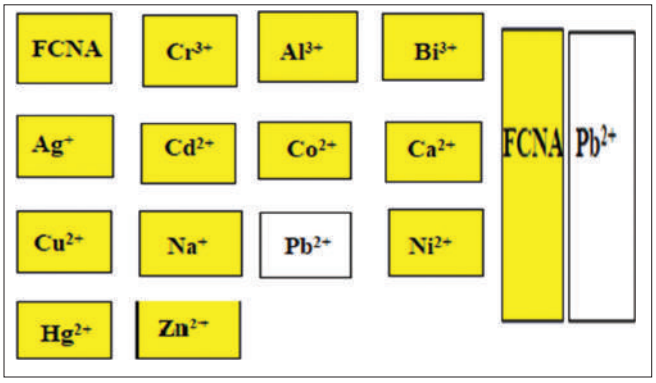

Figure 17: Paper strips of FCNA sensing ability

Application

The application of the sensor is tested with the paper strips, for this application Whatman filter paper 42 is used. The stock solution of the FCNA was prepared $1x10^{-3}$ M concentration. Initially, the Whatman filter paper was soaked into FCNA solution and dried in room temperature. The paper strips are dipped in the different containing metals solution and the colour changes were visually observed only in Pb^{2+} ion from yellow colour to colourless is displayed in Figure 17.

Determination of Pb^{2+} in Real Water and Soil Samples

Soil samples from the semi-arid regions of Ramanad District, Tamil Nadu, were carefully collected to assess the presence of Pb^{2+} ion in environmental conditions. The samples underwent water extraction, ensuring soluble components were effectively separated, followed by centrifugation to remove solid particles and achieve a clear supernatant for further analysis. The extracted solutions were then subjected to pH adjustment, maintaining a range between 4.0 and 8.0, which optimizes conditions for UV-spectrometric analysis and ensures accurate detection of metal ions. To validate the method's accuracy and reliability, a known concentration of Pb^{2+} ion (0.02-0.16 M) was systematically introduced into the prepared samples. The enriched solutions were analysed using spectrometric techniques, with findings presented in Figure 18, demonstrating a strong correlation between the experimentally determined concentrations and theoretical values. This consistency confirms the effectiveness and precision of the approach in detecting Pb^{2+} ion in real-world semi-arid soil samples. Furthermore, these results highlight the environmental relevance of the method, proving its suitability for monitoring heavy metal contamination in soil. Its ability to provide reliable, reproducible data enhances its potential application in environmental assessments, pollution control strategies, and sustainable land management efforts (Divya & Thennarasu, 2020).

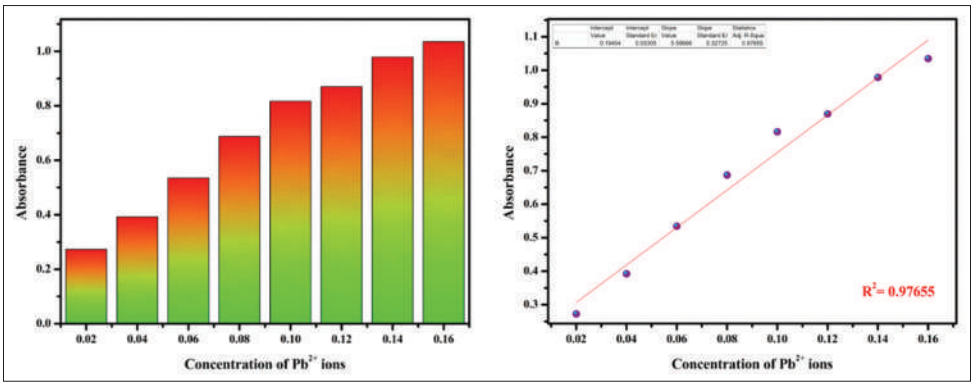

Figure 18: Determination of Pb^{2+} ion in real water samples extracted from soils

CONCLUSION

In conclusion, a chemosensor for the selective detection of lead (Pb^{2+}) ion has been successfully developed. This sensor exhibits high selectivity and sensitivity toward Pb^{2+} ion, with an impressively low detection limit. Studies utilizing FTIR, NMR, and Job's plot suggest that Pb^{2+} ion form complexes with a molar ratio of 2:1. The lower detection limit was determined to be 5.24×10^{-10} M, and the association constant was calculated as $3.22\times10\ M^{-1}$, highlighting the sensor's strong binding affinity for Pb^{2+} ion. Additionally, the ease of synthesis and remarkable selectivity and sensitivity make this chemosensor an effective tool for metal ion detection in the soil samples such arid land and semi-arid land. To validate its practical applications, real sample analysis was performed, demonstrating high reliability. As a result, FCNA proves to be a promising colorimetric chemosensor for detecting heavy metal ions, particularly Pb^{2+} ion, in environmental samples such as arid land and semi-arid land, ensuring its usefulness in pollution monitoring and environmental safety assessments.

ACKNOWLEDGEMENT

We would like to express our sincere thanks to Karpagam Academy of Higher Education for providing Research fellowship, No. KAHE/RS/Ph.D/Fellowship/2024-2025, the necessary infrastructural facilities and laboratory assistance for carrying out this research efficiently.

REFERENCES

Amini, A., Rahimi, M., Behmadi, H., Nazari, M., Benson, V., Cheng, C., & Samali, B. (2020). 2,6-Pyridinedicarbohydrazide-salicylal hydrazone-base derivative with high detection limit and binding constant for emissive ion chemosensing in aqueous solution. *Journal of Photochemistry and Photobiology A: Chemistry, 392*, 112344. https://doi.org/10.1016/j.jphotochem.2019.112344

Burla, S. R., Patil, D. B., Mohana Rao, P., & Jayalakshmi, M. (2013). Delineation of copper (Cu) and zinc (Zn) status in soils of central research station akola. *Journal of Progressive Agriculture, 4*(1), 131-134.

Caballero, A., Espinosa, A., Tárraga, A., & Molina, P. (2008). Ferrocene-based small molecules for dual-channel sensing of heavy- and transition-metal cations. *The Journal of Organic Chemistry, 73*(14), 5489-5497. https://doi.org/10.1021/jo800709v

Cave, M. R., Butler, O., Cook, J. M., Cresser, M. S., Garden, L. M., & Miles, D. L. (2000). Environmental analysis. *Journal of Analytical Atomic Spectrometry, 15*(2), 181-235. https://doi.org/10.1039/b000063i

Chen, C.-T., & Huang, W.-P. (2002). A highly selective fluorescent chemosensor for lead ions. *Journal of the American Chemical Society, 124*(22), 6246-6247. https://doi.org/10.1021/ja025710e

Cho, H., Chae, J. B., & Kim, C. (2018). A thiophene-based blue-fluorescent emitting chemosensor for detecting indium (III) ion. *Inorganic Chemistry Communications, 97*, 171-175. https://doi.org/10.1016/j.inoche.2018.09.037

Choi, J. H., Ryu, J. Y., Park, Y. J., Begum, H., Park, H.-R., Cho, H. J., Kim, Y., & Lee, J. (2014). Fluorescent chemosensor based on pyrrole-aminoindanol for selective zinc detection. *Inorganic Chemistry Communications, 50*, 24-27. https://doi.org/10.1016/j.inoche.2014.10.007

Divya, D., & Thennarasu, S. (2020). A novel isatin-based probe for ratiometric and selective detection of Hg^{2+} and Cu^{2+} ions present in aqueous and environmental samples. *Spectrochimica Acta Part A: Molecular and Biomolecular Spectroscopy, 243*, 118796. https://doi.org/10.1016/j.saa.2020.118796

Durgaparameshwari, M., Kaviya, K., Prabakaran, D. S., Santhamoorthy, M., Rajamanikandan, R., Al-Ansari, M. M., & Mani, K. S. (2024). Designing a simple quinoline-based chromo-fluorogenic receptor for highly specific quantification of copper (II) ions: Environmental and bioimaging applications. *Luminescence, 39*(12), e70068. https://doi.org/10.1002/bio.70068

Dwivedi, R., Singh, S., Chauhan, B. S., Srikrishna, S., Panday, A. K., Choudhury, L. H., & Singh, V. P. (2020). Aroyl hydrazone with large Stokes shift as a fluorescent probe for detection of Cu^{2+} in pure aqueous medium and in vivo studies. *Journal of Photochemistry and Photobiology A: Chemistry, 395*, 112501. https://doi.org/10.1016/j.jphotochem.2020.112501

Elkhatib, E. A., & Moharem, M. L. (2015). Immobilization of copper, lead, and nickel in two arid soils amended with biosolids: Effect of drinking water treatment residuals. *Journal of Soils and Sediments, 15*, 1937-1946. https://doi.org/10.1007/s11368-015-1127-1

Hussain, Z., Bharathamani, D. K., & Subban, R. (2025). Detection of copper ions in arid and semi-arid lands using UV-visible and fluorescence spectrophotometry. *Journal of Aridland Agriculture, 11*, 54-61. https://doi.org/10.25081/jaa.2025.v11.9525

Joshi, D. C. (2016). Adsorption and desorption of copper by calcareous arid soils. *Annals of Arid Zone, 34*(4), 253-257.

Kuo, W.-J., Chen, Y.-H., Jeng, R.-J., Chan, L.-H., Lin, W.-P., & Yang, Z.-M. (2007). Peripheral aryl-substituted pyrrole fluorophores for glassy blue-light-emitting diodes. *Tetrahedron, 63*(30), 7086-7096. https://doi.org/10.1016/j.tet.2007.05.032

Lan, L., Niu, Q., Guo, Z., Liu, H., & Li, T. (2017). Highly sensitive and fast responsive "turn-on" fluorescent sensor for selectively sensing Fe^{3+} and Hg^{2+} in aqueous media based on an oligothiophene derivative and its application in real water samples. *Sensors and Actuators B: Chemical, 244*, 500-508. https://doi.org/10.1016/j.snb.2017.01.042

Leslee, D. B. C., Karuppannan, S., Karmegam, M. V., Gandhi, S., & Subramanian, S. (2018). A fluorescent turn-on carbazole-rhodanine based sensor for detection of Ag^{+} ions and application in Ag^{+} ions imaging in cancer cells. *Journal of Fluorescence, 29*, 75-89. https://doi.org/10.1007/s10895-018-2312-6

Li, X., Feng, S.-S., Wei, Y.-X., & Dong, W.-K. (2022). An investigation of a relatively rigid acyclic salamo-type ligand and its square planar Cu(II) complex. *Journal of Coordination Chemistry, 75*(15-16), 2245-2257. https://doi.org/10.1080/00958972.2022.2123738

Łukasik, N., Wagner-Wysiecka, E., Hubscher-Bruder, V., Michel, S., Bocheńska, M., & Kamińska, B. (2016). Naphthyl- vs. anthrylpyridine-2,6-dicarboxamides in cation binding studies. Synthesis and spectroscopic properties. *Supramolecular Chemistry, 28*(7-8), 673-685. https://doi.org/10.1080/10610278.2015.1119830

Maloney, B., Bayon, B. L., Zawia, N. H., & Lahiri, D. K. (2018). Latent consequences of early-life lead (Pb) exposure and the future: Addressing the Pb crisis. *NeuroToxicology, 68*, 126-132. https://doi.org/10.1016/j.neuro.2018.06.016

Maurya, N., & Singh, A. K. (2017). Indirect approach for CN^{-} detection via Cu^{2+} induced turn-off sensor: Using novel AIEE fluorophore with logic gate and antimicrobial application. *Dyes and Pigments, 147*, 484-490. https://doi.org/10.1016/j.dyepig.2017.08.046

Novikov, A. S. (2022). Non-covalent interactions in coordination and organometallic chemistry. *Crystals, 10*(6), 537. https://doi.org/10.3390/cryst10060537

Pothulapadu, C. A. S., Jayaraj, A., Swathi, N., Priyanka, R. N., & Sivaraman G. (2021). Novel benzothiazole-based highly selective ratiometric fluorescent Turn-On sensors for Zn^{2+} and colorimetric chemosensors for Zn^{2+}, Cu^{2+}, and Ni^{2+} ions. *ACS Omega, 6*(38), 24473-24483. https://doi.org/10.1021/acsomega.1c02855

Prabhu, J., Velmurugan, K., & Nandhakumar, R. (2015). Development of fluorescent lead II sensor based on an anthracene derived chalcone. *Spectrochimica Acta Part A: Molecular and Biomolecular Spectroscopy, 144*, 23-28. https://doi.org/10.1016/j.saa.2015.02.028

Rahimi, H., Hosseinzadeh, R., & Tajbakhsh, M. (2020). A new and efficient pyridine-2,6-dicarboxamide-based fluorescent and colorimetric chemosensor for sensitive and selective recognition of Pb^{2+} and Cu^{2+}. *Journal of Photochemistry and Photobiology A: Chemistry*, *407*, 113049. https://doi.org/10.1016/j.jphotochem.2020.113049

Rasmussen, S. C., Evenson, S. J., & McCausland, C. B. (2015). Fluorescent thiophene-based materials and their outlook for emissive applications. *Chemical Communications, 51*(22), 4528-4543. https://doi.org/10.1039/c4cc09206f

Roy, A., Shee, U., Mukherjee, A., Mandal, S. K., & Roy, P. (2019). Rhodamine-

based dual chemosensor for Al^{3+} and Zn^{2+} ions with distinctly separated excitation and emission wavelengths. *ACS Omega, 4*(4), 6864-6875. https://doi.org/10.1021/acsomega.9b00475

Rupa, S. A., Moni, M. R., Patwary, M. A. M., Mahmud, M. M., Haque, M. A., Uddin, J., & Abedin, S. M. T. (2022). Synthesis of novel tritopic hydrazone ligands: spectroscopy, biological activity, DFT, and molecular docking studies. *Molecules, 27*(5), 1656. https://doi.org/10.3390/molecules27051656

Santhamoorthy, M., Mani, K. S., Periyasami, G., Kim, S.-C., Mohan, A., & Phan, T. T. V. (2024). Synthesis and surface modifications of mesoporous silica adsorbent for selective removal of chromium (Cr^{3+}) ions from wastewater. *Separation Science and Technology, 59*(4), 547-560. https://doi.org/10.1080/01496395.2024.2335345

Shoora, S. K., Jain, A. K., & Gupta, V. K. (2015). A simple Schiff base based novel optical probe for aluminium (III) ions. *Sensors and Actuators B: Chemical, 216*, 86-104. https://doi.org/10.1016/j.snb.2015.04.038

Suaad, K. A., Zeina Gany, F., & Sherin Mohammed, M. (2020). Determination of copper and lead in soil samples and cultivated plants in Al-muradiya area, Iraq. *Plant Archives, 20*(2), 7461-7464.

Sun, T., Niu, Q., Li, Y., Li, T., & Liu, H. (2017). Novel oligothiophene-based dual-mode chemosensor: "naked-eye" colorimetric recognition of Hg^{2+} and sequential off-on fluorescence detection of Fe^{3+} and Hg^{2+} in aqueous media and its application in practical samples. *Sensors and Actuators B: Chemical, 248*, 24-34. https://doi.org/10.1016/j.snb.2017.03.128

Sun, X., Wang, Y.-W., & Peng, Y. (2012). A selective and ratiometric bifunctional fluorescent probe for Al^{3+} ion and proton. *Organic Letters, 14*(13), 3420-3423. https://doi.org/10.1021/ol301390g

Tahmasebi, E., Masoomi, M. Y., Yamini, Y., & Morsali, A. (2014). Application of mechanosynthesized azine-decorated zinc(II) metal–organic frameworks for highly efficient removal and extraction of some heavy-metal ions from aqueous samples: A comparative study. *Inorganic Chemistry, 54*(2), 425-433. https://doi.org/10.1021/ic5015384

Torawane, P., Tayade, K., Bothra, S., Sahoo, S. K., Singh, N., Borse, A., & Kuwar, A. (2015). A highly selective and sensitive fluorescent 'turn-on' chemosensor for Al^{3+} based on CN isomerisation mechanism with nanomolar detection. *Sensors and Actuators B: Chemical, 222*, 562-566. https://doi.org/10.1016/j.snb.2015.08.104

Udhayakumari, D., & Velmathi, S. (2013). Colorimetric chemosensor for multi-signaling detection of metal ions using pyrrole based Schiff bases. *Spectrochimica Acta Part A: Molecular and Biomolecular Spectroscopy, 122*, 428-435. https://doi.org/10.1016/j.saa.2013.11.083

Velmathi, S., Reena, V., Suganya, S., & Anandan, S. (2011). Pyrrole based Schiff bases as colorimetric and fluorescent chemosensors for fluoride and hydroxide anions. *Journal of Fluorescence, 22*, 155-162. https://doi.org/10.1007/s10895-011-0942-z

Wang, A., Fan, R., Dong, Y., Song, Y., Zhou, Y., Zheng, J., Du, X., Xing, K., & Yang, Y. (2017a). Novel hydrogen-bonding cross-linking aggregation-induced emission: water as a fluorescent "ribbon" detected in a wide range. *ACS Applied Materials & Interfaces, 9*(18), 15744-15757. https://doi.org/10.1021/acsami.7b01254

Wang, Y., Mao, P.-D., Wu, W.-N., Mao, X.-J., Fan, Y.-C., Zhao, X.-L., Xu, Z.-Q., & Xu, Z.-H. (2017b). New pyrrole-based single-molecule multianalyte sensor for Cu^{2+}, Zn^{2+}, and Hg^{2+} and its AIE activity. *Sensors and Actuators B: Chemical, 255*, 3085-3092. https://doi.org/10.1016/j.snb.2017.09.133

Xiang, Y., Tong, A., Jin, P., & Ju, Y. (2006). New fluorescent rhodamine hydrazone chemosensor for Cu(II) with high selectivity and sensitivity. *Organic Letters, 8*(13), 2863-2866. https://doi.org/10.1021/ol0610340